J. Chem. Thermodynamics 175 (2022) 106897

Contents lists available at ScienceDirect

The Journal of Chemical Thermodynamics

journal homepage: www.journals.elsevier.com/the-journal-of-chemical-thermodynamics

Influence of high pressure on the solubility of ribavirin in six pure solvents from 283.15 to 323.15 K

Yaoguang Feng [a], Hongxun Hao [a,b,c], Beiqian Tian [a], Kui Chen [a], Na Wang [a,b], Ting Wang [a,b,*], Xin Huang [a,b,d,*]

[a] National Engineering Research Center of Industrial Crystallization Technology, School of Chemical Engineering and Technology, Tianjin University, Tianjin 300072, China
[b] Collaborative Innovation Center of Chemical Science and Engineering (Tianjin), Tianjin 300072, China
[c] School of Chemical Engineering and Technology, Hainan University, Haikou 570228, China
[d] Zhejiang Institute of Tianjin University, Ningbo, Zhejiang 315201, China

ARTICLE INFO

Keywords:
Ribavirin
Solubility
High pressure
Solvation free energy
Thermodynamic properties

ABSTRACT

The solubility of ribavirin in six pure solvents was measured at 9.0 MPa and 0.1 MPa to evaluate the influence of high pressure on solubility at the temperature range from 283.15 K to 323.15 K. The results indicated that all the solubilities of ribavirin decreased slightly at 9.0 MPa compared with those at 0.1 MPa. Solvation free energy of ribavirin in six solvents under two pressures was calculated to explain the decrease of solubility under high pressure. Besides, the solubility of ribavirin increased with the rising temperature under both 0.1 MPa and 9.0 MPa. Furthermore, the experimental solubility data under two pressures were correlated by the modified Apelblat equation and NRTL model. The average relative deviation (ARD%) value of the modified Apelblat equation is less than 3 %, which can give better correlation results. Finally, the thermodynamic properties of mixing and dissolution of ribavirin in six pure solvents under two pressures were also calculated based on the solubility experimental data and the NRTL equation.

1. Introduction

Ribavirin ($C_8H_{12}N_4O_5$, CAS Registry No. 36791–04-5, Fig. 1) is a water-soluble antiviral compound widely used for treating hepatitis C virus infections, respiratory syncytial virus infections, and Lassa fever virus infections.[1–3] At the moment, the synthetic methods of ribavirin include chemical and microbiological approaches, both of which need solution recrystallization.[4] Ribavirin was previously reported to have two single-crystalline forms, conventionally referred to as thermodynamically stable Form I and metastable enantiotropic Form II.[5–7] Form II has a low melting point (T_m = 441.3 K ± 0.7 K) and density (1.587 g/cm^3), while Form I has a higher melting point and density, 450.5 K ± 0.2 K and 1.653 g/cm^3, respectively.[5] These two different crystal forms of ribavirin can be prepared by recrystallization from different solvents.[5] As the metastable enantiotropic, Form II has higher solubility and bioavailability than Form I, which is also the commercially available polymorph.

Crystallization is widely applied in the pharmaceutical industry as a separation and purification operation. The selection of solvents in crystallization will affect the purity, crystal polymorphism, morphology, and yield of the final products.[8,9] Therefore, it is important to obtain the solubility data of ribavirin in different solvents. However, there are few studies on the solubility of ribavirin, and only the solubility of ribavirin Form II in several binary solvents and several pure solvents was reported.[10,11] To supply a sufficient database for the selection of crystallization methods and solvents, it is necessary to determine the solubility of ribavirin Form II in other pure solvents.

In addition, most studies have always been focused on solubility variation with the temperature at atmospheric pressure, but the effect of pressure on solubility is usually ignored. However, this effect may become significant under high pressure.[12] Seiji et al. measured the solubility of ammonium chloride in water under the pressure from 0.10 to 300 MPa and it was found that the solubility of ammonium chloride decreased with the increase in pressure.[13] In addition, as the basic data of pressure-induced crystallization, the solubility of ribavirin in pure solvents under high pressure is essential to the optimization of the crystallization process. Therefore, the effects of pressure and temperature on solubility should be evaluated simultaneously.

* Corresponding authors.
E-mail addresses: wang_ting@tju.edu.cn (T. Wang), x_huang@tju.edu.cn (X. Huang).

https://doi.org/10.1016/j.jct.2022.106897
Received 30 January 2022; Received in revised form 9 August 2022; Accepted 11 August 2022
Available online 13 August 2022
0021-9614/

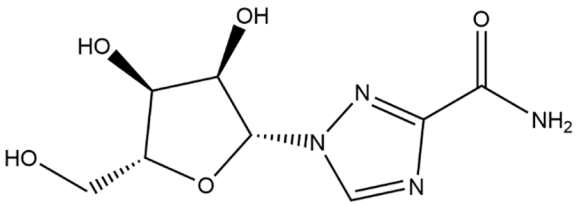

Fig. 1. Chemical structure of ribavirin.

The solubility data of ribavirin (Form II) was measured at 9.0 MPa and atmospheric pressure (0.1 MPa) to evaluate the effect of high pressure on the solubility, and 9.0 MPa is a proper value that is easy to be achieved in industry.[14,15] The solubility experiment was carried out from 283.15 K to 323.15 K and this temperature range is easy to control and can be realized in industry.[16,17] Besides, the ribavirin could be stable under this temperature condition. The selected solvents were water, ethylene glycol, 1,2-propanediol, *n*-methylpyrrolidone, dimethylformamide, and dimethylacetamide because after trying many common solvents in the preliminary experiment, it was found that these six solvents had good solubility to ribavirin, and these six solvents have the potential advantage in the actual industrial production of ribavirin.

Besides, the solvation free energy of ribavirin in six solvents under two pressures was calculated to explain the difference in solubility. In addition, the modified Apelblat equation and the NRTL model were applied to correlate the relationship between temperature and solubility of ribavirin under two pressures. Finally, thermodynamic properties under two pressures, including the Gibbs free energy, the enthalpy, and the entropy in the process of mixing and dissolution, were calculated based on the experimental solubility data and the NRTL model.

2. Experimental

2.1. Materials

The materials used in this study are listed in Table 1. Ribavirin (mass purity ≥ 99.0 %) was obtained from Shanghai Xianding Biotechnology Co., ltd. *N*-methylpyrrolidone was obtained from Shanghai Bide Pharmaceutical Technology Co., ltd. Ultrapure water (18.2 MΩ•cm in resistivity) was prepared in our laboratory with Nanopure Water Purifier (Thermo Scientific, US). The other solvents were obtained from Lianlong Bohua Chemical Co., ltd. All the materials were used directly without further purification.

2.2. Characterization methods

The X-ray powder diffractometer (D/max-2500, Rigaku, Japan) was used to characterize the crystal form of ribavirin after each experiment, to check whether there was polymorph transformation of ribavirin during solubility determination. The samples were scanned from 2° to 40° at a diffraction angle (2θ) with a scanning rate of 8°/min. The voltage was 40 kV and the current was 100 mA.

The Differential Scanning Calorimeter (DSC 1/500, Mettler-Toledo, Switzerland) was used to determine the melting temperature (T_m) and fusion enthalpy ($\Delta_{fus}H$) of ribavirin. Indium calibration standard sample (T_m = 429.75 K, $\Delta_{fus}H$ = 3.286 kJ/mol[18]) was used to calibrate the temperature and heat flow of DSC. About 8 mg sample of ribavirin was added into an aluminum pan and accurately weighed by an analytical balance (AE204S, Mettler Toledo, Switzerland) with an uncertainty of ± 0.00001 g. The measurement was performed in a temperature range of 298.15 K to 473.15 K at a heating rate of 10 K/min in a high-purity nitrogen atmosphere.

2.3. Solubility measurements

The solubility of ribavirin at 0.1 MPa and 9.0 MPa was measured by the gravimetric method.[19,20] The solubility at 9.0 MPa was measured using a 100 ml-high pressure stainless steel reactor (Xi'an Taikang Biotechnology Co., ltd, China), whose design pressure was 10.0 MPa. As shown in Fig. 2, the reactor was equipped with an inflation valve, liquid taking valve, magnetic stirrer, and jacket. In addition, the reactor was equipped with a sapphire window to observe the dissolution of ribavirin.

Fig. 2. High-pressure solubility experimental device.

Table 1
The source and purity of materials used in the experiment.

Chemical name	CAS Registry No.	Source	Mass purity	Analysis method
Ribavirin	36791–04-5	Xianding Biotechnology Co., ltd., Shanghai, China	≥ 0.990	HPLC[a]
Water	7732–18-5	Lab-made		
Ethylene glycol	107–21-1	Lianlong Bohua Chemical Co., ltd., Tianjin, China	≥ 0.995	GC[b]
1,2-propanediol	57–55-6	Lianlong Bohua Chemical Co., ltd., Tianjin, China	≥ 0.990	GC[b]
N-methylpyrrolidone	872–50-4	Bide Pharmaceutical Technology Co., ltd., Shanghai, China	≥ 0.998	GC[b]
Dimethylformamide	68–12-2	Lianlong Bohua Chemical Co., ltd., Tianjin, China	≥ 0.995	GC[b]
Dimethy[a]lacetamide	127–19-5	Lianlong Bohua Chemical Co., ltd., Tianjin, China	≥ 0.990	GC[b]

The analytical method and purity are obtained from the reagent company.
All the materials were used directly without further purification.
[a] High-performance liquid chromatography. [b] Gas chromatography.

The high pressure was achieved by the aeration of nitrogen using a nitrogen steel cylinder (Tianjin Liufang Industrial Gas Distribution Co., ltd.). The nitrogen purity ≥ 99.999 % and the initial pressure ≥ 14.5 MPa. The reason why nitrogen was selected as the pressure transmission medium was that it has the advantages of inertia and safety.

The solubility under atmospheric pressure was measured using a 100 ml-glass jacketed crystallizer (Tianjin Yipujia Technology Co., ltd., China). The crystallizer was equipped with a magnetic stirrer (Tianjin Ounuo Instrument Co., ltd., China) to control the stirring rate. The temperature of the reactor and crystallizer was controlled by a thermostat (Nanjing Xianou Laboratory Instrument Works Co., ltd., China) with a temperature accuracy of ± 0.01 K. Since solubility measurement is a very common experiment, the measurement process, and solubility method validation were briefly described in the supplementary materials. As shown in Fig. S1, the dissolution equilibrium can be reached faster under 9.0 MPa than under 0.1 MPa.

2.4. Solvation free energy

The solvation free energy of a molecule is defined as the energy required for the solute to transfer from the gas phase to the solution at constant temperature and constant pressure, which reflects the interaction between solvent and solute.[21] The larger the absolute value of the solvation free energy, the higher solubility in general.[22] The solvation free energy can be calculated with the Forcite module of Materials Studio software (Accelrys Software Inc., US), and the calculation steps in this work are briefly as follows:[23,24].

Firstly, the structures of ribavirin and solvent molecules were constructed and geometrically optimized. The molecular structure of ribavirin (Form II) was obtained from Cambridge Crystallographic Data Centre (CCDC Number: 1284474). The structures of solvent molecules were sketched by Material Studio. Then, an amorphous cell containing one ribavirin molecule and 500 solvent molecules was constructed under the external pressures of 0.1 MPa and 9.0 MPa, respectively. After the geometry optimization, the amorphous cell was equilibrated with 1000 ps NPT dynamics. Here NPT refers to the constant-particle number, constant-pressure, and constant-temperature ensemble. The simulated temperature was 298.15 K, and the pressure was 0.1 MPa and 9.0 MPa respectively. Finally, the solvation free energy was calculated, and the results were given directly by the software.

3. Thermodynamic models and thermodynamic properties

3.1. Modified Apelblat equation

The modified Apelblat equation with three parameters is a commonly used semi-empirical model for correlating the relationship between solute solubility and temperature. The formula is as follows.[25].

$$\ln x_1 = A + \frac{B}{T} + C\ln T \tag{1}$$

where x_1 represents the mole fraction solubility of ribavirin. A, B, and C are model parameters. T is the absolute temperature in Kelvin.[26].

3.2. NRTL model

The nonrandom two-liquid (NRTL) model proposed by Renon and Prausnitz in 1968 is a general thermodynamic model to describe solute solubility, which can be expressed as follows.[27,28].

$$\ln x_1 = \frac{\Delta fusH}{R}\left(\frac{1}{T_m} - \frac{1}{T}\right) - \ln\gamma_1 \tag{2}$$

$$\ln\gamma_1 = x_2^2\left[\frac{\tau_{21}G_{21}^2}{(x_1 + G_{21}x_2)^2} + \frac{\tau_{12}G_{12}^2}{(x_2 + G_{12}x_1)^2}\right] \tag{3}$$

$$G_{12} = e^{(-\alpha\tau_{12})} \tag{4}$$

$$G_{21} = \mathrm{e}^{(-\alpha\tau_{21})} \tag{5}$$

$$\tau_{12} = \frac{g_{12} - g_{22}}{RT} = \frac{\Delta g_{12}}{RT} \tag{6}$$

$$\tau_{21} = \frac{g_{21} - g_{11}}{RT} = \frac{\Delta g_{21}}{RT} \tag{7}$$

where x_1, $\Delta_{fus}H$, R, T_m, T, and γ_1 are the molar fraction solubility of the solute, the fusion enthalpy of the solute, the gas constant, the melting point of the solute, the absolute temperature in Kelvin, and the activity coefficient, respectively.[9] Δg_{12}, Δg_{21}, and α are model parameters of the NRTL equation. The parameter α represents the non-randomness and noideality of the solution, and its value is between 0 and 1.[29] In this work, the value of α was determined by the enumeration method until a better fitting quality with the experimental value was obtained.[30].

3.3. Mixing and dissolution thermodynamic properties

To understand the influence of pressure on the mixing and dissolution process, the thermodynamic properties of mixing and dissolution were calculated. For the mixing process in the real solution system, the Gibbs energy, enthalpy, and entropy can be calculated by the following Eqs. (8–10).

$$\Delta_{mix}G = G^E + RT(x_1\ln x_1 + x_2\ln x_2) \tag{8}$$

$$\Delta_{mix}H = H^E \tag{9}$$

$$\Delta_{mix}S = S^E - R(x_1\ln x_1 + x_2\ln x_2) \tag{10}$$

where x_1 and x_2 are the mole fraction of solute and corresponding pure solvent respectively. G^E, H^E, and S^E are the excess mixing properties of Gibbs energy, enthalpy, and entropy, which can be calculated by Eqs. (11–13).[31].

$$G^E = RT(x_1\ln\gamma_1 + x_2\ln\gamma_2) \tag{11}$$

$$H^E = -T^2\left[\frac{\partial(G^E/T)}{\partial T}\right] = -RT^2\left[x_1\left(\frac{\partial\ln\gamma_1}{\partial T}\right)_{p,x} + x_2\left(\frac{\partial\ln\gamma_2}{\partial T}\right)_{p,x}\right] \tag{12}$$

$$\Delta_{mix}S = \frac{\Delta_{mix}H - \Delta_{mix}G}{T} \tag{13}$$

where γ_1 and γ_2 represent the activity coefficient of solute and pure solvent, respectively, which can be obtained from the NRTL model.

Based on the thermodynamic properties of mixing, the thermodynamics of dissolution can be approximately calculated by the following equations.[32].

$$\Delta_{dis}H = x_N\Delta_{fus}H + \Delta_{mix}H \tag{14}$$

$$\Delta_{dis}S = x_N\Delta_{fus}S + \Delta_{mix}S \tag{15}$$

$$\Delta_{dis}G = \Delta_{dis}H - T\Delta_{dis}S \tag{16}$$

where $\Delta_{fus}H$ and $\Delta_{fus}S$ represent the fusion enthalpy and entropy, respectively. The value of $\Delta_{fus}H$ can be determined by the DSC method. And the value of $\Delta_{fus}S$ can be calculated from Eq. (17) because $\Delta_{fus}G$ can be regarded as zero in the melting equilibrium.

$$\Delta_{fus}S = \frac{\Delta_{fus}H}{T_m} \tag{17}$$

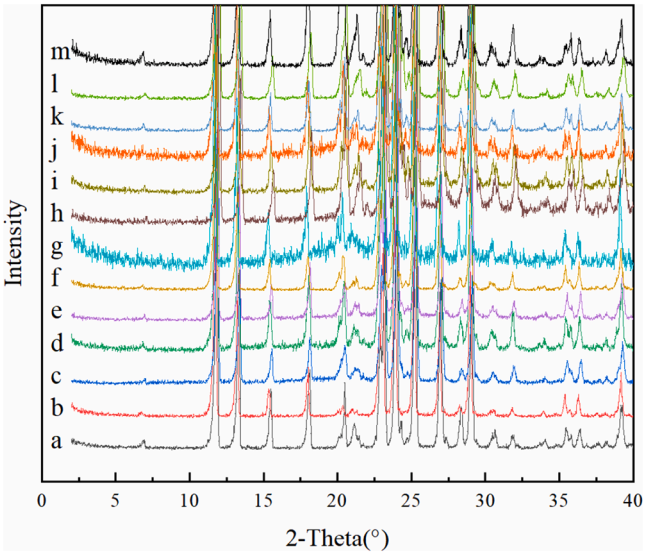

Fig. 3. Powder X-ray diffraction patterns of residual solids in different solvents: (a) raw ribavirin, (b-g) residual solids in water, ethylene glycol, 1,2-propanediol, *n*-methylpyrrolidone, dimethylformamide, and dimethylacetamide at 0.1 MPa, (h-m) residual solids in water, ethylene glycol, 1,2-propanediol, *n*-methylpyrrolidone, dimethylformamide, and dimethylacetamide at 9.0 MPa.

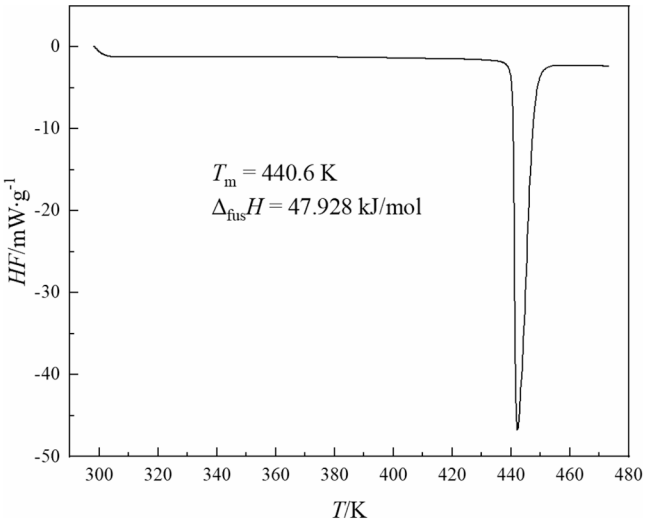

Fig. 4. DSC plot of ribavirin (Form II) raw material.

In this work, the calculated values of solubility as well as the model parameters in modified Apelblat and NRTL models, and the mixing and dissolution thermodynamic properties, were calculated in MATLAB (MathWorks.Inc, US).

4. Results and discussion

4.1. Characterization of ribavirin

The PXRD patterns of the ribavirin raw material and undissolved wet solid are compared and illustrated in Fig. 3. It can be seen that these spectrograms are consistent, which means that all the samples are the same in polymorph (Form II). Thus, there was no polymorphic transformation or solvate formation during the solubility experiments under two pressures.

The DSC analysis results of ribavirin raw material include melting point (T_m, the onset temperature of the melting process) and enthalpy of

Table 2
Experimental and calculated values of mole fraction solubility of crystalline ribavirin (Form II) in six pure solvents from 283.15 K to 323.15 K at 0.1 MPa and 9.0 MPa.[a,b,c,d]

T/K	$10^3x_1^{exp\text{-}A}$	$10^3x_1^{exp\text{-}H}$	Apelblat $10^3x_1^{cal\text{-}A}$	Apelblat $10^3x_1^{cal\text{-}H}$	NRTL $10^3x_1^{cal\text{-}A}$	NRTL $10^3x_1^{cal\text{-}H}$
Water						
283.15	5.43	4.88	5.13	4.81	4.39	3.89
288.15	6.25	5.95	6.52	6.00	6.04	5.35
293.15	7.93	7.34	8.35	7.58	8.20	7.28
298.15	10.9	10.1	10.8	9.70	11.0	9.79
303.15	14.4	12.2	14.0	12.5	14.6	13.1
308.15	18.5	16.6	18.4	16.4	19.3	17.2
313.15	25.1	21.6	24.2	21.6	25.1	22.5
318.15	32.6	29.3	32.1	28.7	32.3	29.0
323.15	41.4	37.7	42.8	38.5	41.3	37.1
Ethylene glycol						
283.15	6.40	5.94	6.21	5.84	6.00	5.66
288.15	6.84	6.53	6.84	6.48	6.75	6.41
293.15	7.46	7.18	7.71	7.35	7.67	7.30
298.15	8.44	8.13	8.89	8.49	8.85	8.43
303.15	10.5	9.97	10.5	9.99	10.6	10.0
308.15	13.3	12.7	12.5	11.9	12.9	12.2
313.15	16.0	14.8	15.3	14.5	15.6	14.6
318.15	19.0	17.8	19.0	17.9	19.0	17.8
323.15	23.1	21.8	23.9	22.3	23.5	22.2
1,2-propanediol						
283.15	2.81	2.77	2.72	2.70	1.94	1.86
288.15	3.01	2.98	3.08	3.01	2.38	2.27
293.15	3.52	3.48	3.56	3.43	2.96	2.82
298.15	4.09	4.01	4.17	3.98	3.69	3.49
303.15	4.86	4.77	4.97	4.69	4.61	4.36
308.15	6.23	5.61	6.01	5.63	5.88	5.44
313.15	7.64	7.04	7.37	6.87	7.47	6.96
318.15	9.37	8.79	9.14	8.49	9.52	8.94
323.15	11.0	10.3	11.5	10.6	12.0	11.2
N-methylpyrrolidone						
283.15	99.3	98.6	99.2	98.4	99.0	98.6
288.15	100	99.6	100	99.5	100	99.5
293.15	102	101	102	101	102	101
298.15	105	103	105	104	105	104
303.15	108	107	109	107	108	107
308.15	113	112	113	112	113	111
313.15	119	117	118	117	118	116
318.15	124	123	124	122	124	122
323.15	131	128	131	129	132	130
Dimethylformamide						
283.15	41.7	39.7	41.3	39.4	41.7	39.9
288.15	42.0	40.2	42.2	40.5	42.3	40.5
293.15	43.2	41.7	43.8	42.0	43.5	41.7
298.15	45.6	44.1	45.9	44.1	45.6	43.7
303.15	48.9	46.7	48.7	46.7	48.5	46.3
308.15	52.7	50.2	52.2	50.1	52.1	49.7
313.15	57.0	54.5	56.6	54.1	56.5	54.0
318.15	62.1	58.7	61.8	58.9	62.0	59.0
323.15	67.3	64.5	68.1	64.7	68.3	65.3
Dimethylacetamide						
283.15	73.3	71.4	73.6	71.5	76.8	75.1
288.15	76.5	74.5	76.4	74.4	77.1	75.2
293.15	79.7	77.7	79.4	77.5	78.3	76.2
298.15	82.9	80.4	82.6	80.6	80.5	78.2
303.15	86.4	83.7	86.0	83.7	83.5	80.9
308.15	89.5	86.7	89.5	87.0	87.5	84.6
313.15	92.5	90.5	93.3	90.3	92.5	89.1
318.15	96.3	93.8	97.3	93.7	98.3	94.6
323.15	103	97.0	102	97.1	105	101

[a] Standard uncertainty of temperature is $u(T) = 0.05$ K. Relative standard uncertainty of the solubility measurement is $u_r(x_1) = 0.05$.
[b] Standard uncertainty of pressure at 0.1 MPa is $u(p) = 0.3$ kPa.
[c] Standard uncertainty of pressure at 9.0 MPa is $u(p) = 50$ kPa.
[d] $x_1^{exp\text{-}A}$ and $x_1^{exp\text{-}H}$ are the experimental mole fraction solubility at 0.1 MPa and 9.0 MPa, respectively. $x_1^{cal\text{-}A}$ and $x_1^{cal\text{-}H}$ are the calculated mole fraction solubility at 0.1 MPa and 9.0 MPa, respectively.

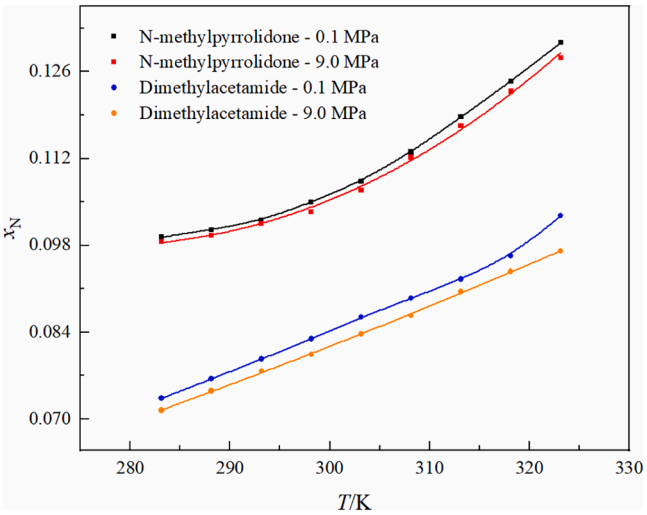

Fig. 5. Mole fraction solubility of crystalline ribavirin (Form II) in *n*-methylpyrrolidone and dimethylacetamide at temperatures ranging from 283.15 K to 323.15 K at 0.1 MPa and 9.0 MPa: symbol - experimental value, curve - calculated by the modified Apelblat model.

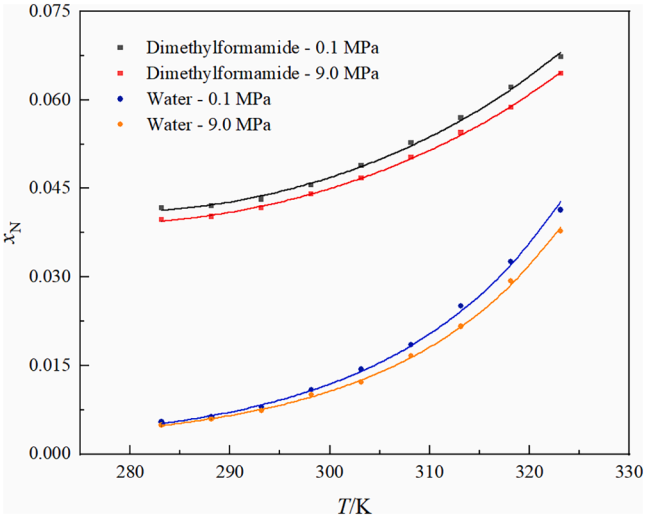

Fig. 6. Mole fraction solubility of crystalline ribavirin (Form II) in dimethylformamide and water at temperatures ranging from 283.15 K to 323.15 K at 0.1 MPa and 9.0 MPa: symbol - experimental value, curve - calculated by the modified Apelblat model.

fusion ($\Delta_{fus}H$), as shown in Fig. 4. The T_m and $\Delta_{fus}H$ are 440.6 K and 47.928 kJ/mol, respectively. This is almost consistent with the reported data, T_m = 441.3 K and $\Delta_{fus}H$ = 44.320 kJ/mol reported by Vasa[5], T_m = 441.2 K and $\Delta_{fus}H$ = 45.700 kJ/mol reported by Kohsaku[33]. However, there is a slight deviation between our measurement results and the reported values, which may be caused by the differences in raw material sources, test instruments, test methods, or experimental environment. The standard uncertainties of the T_m and $\Delta_{fus}H$ are 0.5 K and 0.96 kJ/mol, respectively.

It should be pointed out that in ref. [11], the T_m and $\Delta_{fus}H$ were 445.5 K and 28.290 kJ/mol respectively, which is quite different from the data measured in this work and other references. Because the onset point was not 445.5 K as the author declared according to the DSC curve in ref. [11], it can be considered that the melting parameters including T_m and $\Delta_{fus}H$ in ref. [11] may be wrong.

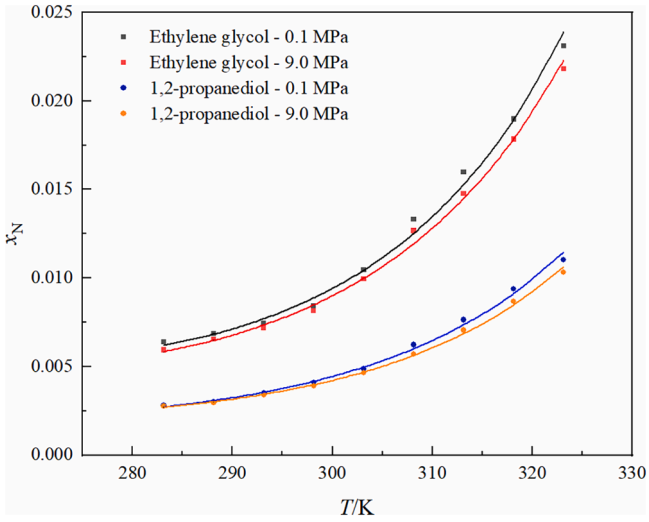

Fig. 7. Mole fraction solubility of crystalline ribavirin (Form II) in ethylene glycol and 1,2-propanediol at temperatures ranging from 283.15 K to 323.15 K at 0.1 MPa and 9.0 MPa: symbol - experimental value, curve - calculated by the modified Apelblat model.

Table 3
Solvation free energy of crystalline ribavirin (Form II) in six pure solvents.

Solvent	Solvation free energy/kJ·mol^{-1}	
	Calculated at 0.1 MPa	Calculated at 9.0 MPa
Water	−74.533	−63.667
1,2-propanediol	−95.387	−89.594
Ethylene glycol	−94.680	−83.529
N-methylpyrrolidone	−89.720	−82.482
Dimethylformamide	−85.425	−79.037
Dimethylacetamide	−92.775	−88.744

4.2. Solubility data of ribavirin

The mole fraction solubility data of ribavirin in six pure solvents at 9.0 MPa and 0.1 MPa and temperatures in the range of 283.15 K to 323.15 K are presented in Table 2 and graphically shown in Figs. 5-7. It was indicated that the solubility at each temperature of ribavirin decreases slightly at 9.0 MPa compared with that at 0.1 MPa, and with the increase in temperature, this decreasing trend is more obvious. As shown in Fig. S1, the dissolution equilibrium can be reached faster under 9.0 MPa than under 0.1 MPa. Hildebrand predicted that the solubility decreased with the increase of pressure according to the regular solution theory in the 1950 s, which is consistent with our experimental results. [26].

It should be pointed out that no validation with well-studied systems were conducted for the high-pressure apparatus. In addition, it was assumed that the dissolved gas has no effect on the reported solubility since this effect was difficult to assess.

The decrease in solubility may be due to the limitation of solute molecular movement in the solution system under high pressure. In addition, the solvation free energy of ribavirin in six pure solvents was calculated under two pressure and the results were listed in Table 3. The calculated results show that the absolute value of solvation free energy under high pressure is lower than that under atmospheric pressure, which is consistent with the experimental results. In other words, high pressure is not conducive to the solvation of solutes.

Solvent properties were collected from the literature to explain the solubility difference in solvents, as summarized in Table 4. It was supposed that pressure has a great influence on the solubility of ribavirin in dimethylacetamide, dimethylformamide, and water. However, this result is not completely consistent with the compressibility order of

Table 4
Physicochemical properties of selected solvents and other alcohol solvents.[a]

Solvent	κ_T[b]	π[c]	$\sum\alpha$[d]	$\sum\beta$[e]	Dipole moment[f]	Cohesive energy density[g]
Water	0.457	1.09	1.17	0.47	1.87	2095.9
1,2-propanediol	0.392	0.76				
Ethylene glycol	0.487	0.92	0.90	0.52	2.28	857.86
N-methylpyrrolidone	0.642	0.92	0.00	0.77	4.10	518.28
Dimethylformamide	0.630	0.88	0.00	0.74	3.82	463.96
Dimethylacetamide	0.620	0.85	0.00	0.78	3.70	439.94
Methanol	1.248	0.60	0.43	0.47	1.70	808.26
Ethanol	1.153	0.54	0.37	0.48	1.69	618.87
N-propanol	1.025	0.52	0.37	0.48	1.55	520.37
N-butanol	0.941	0.47	0.37	0.48	1.66	446.01
Sec-butanol	0.983	0.40	0.33	0.56	1.80	416.88

[a] Obtained from refs.[35,36].
[b] Isothermal compressibility, in the unit of GPa^{-1}.
[c] Polarity/dipolarity of the pure solvent.
[d] Summation of the hydrogen bond donor propensities of the pure solvent.
[e] Summation of the hydrogen bond acceptor propensities of the pure solvent.
[f] Dipole moment in the unit of debye.
[g] Cohesive energy density in the unit of $J \cdot cm^{-3}$.

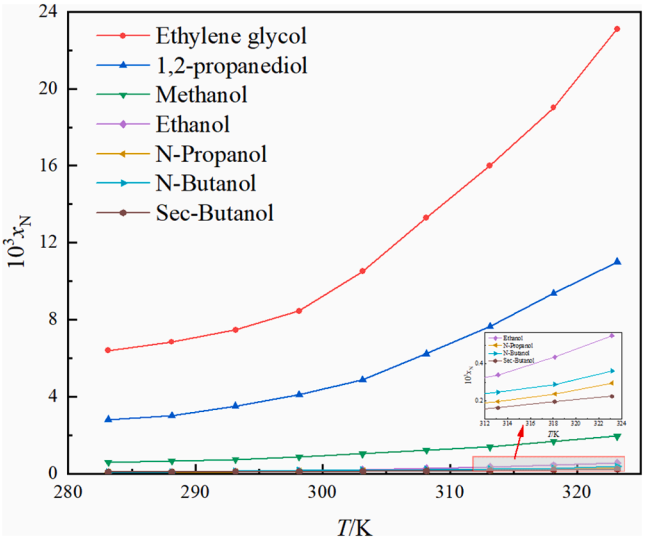

Fig. 8. Mole fraction solubility of crystalline ribavirin (Form II) in alcohol solvents at 0.1 MPa. The solubility data in ethylene glycol and 1,2-propanediol were measured by this work, and the solubility data in other alcohol solvents were obtained from ref. [11].

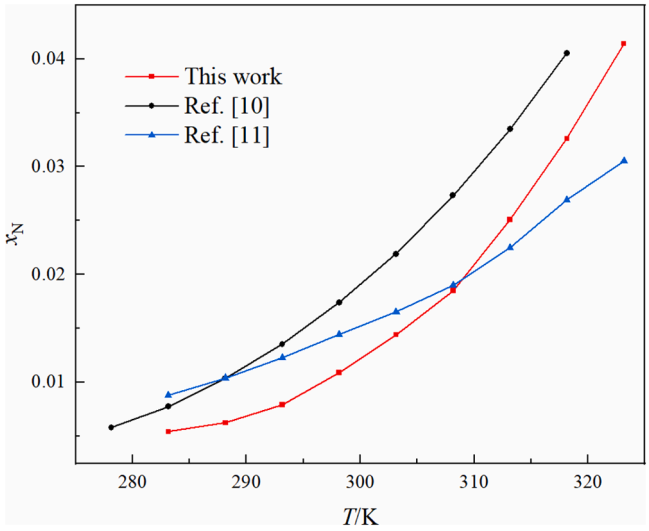

Fig. 9. Mole fraction solubility of crystalline ribavirin (Form II) in water at atmospheric pressure in this work and refs. [10–11].

solvents.

The effect of pressure on solubility values was weaker compared to temperature. With the temperature increasing, the solubility of ribavirin in each solvent increased significantly. In this study, the average solubility in these solvents are ranked as *n*-methylpyrrolidone > dimethylacetamide > dimethylformamide > water > ethylene glycol > 1,2-propanediol. However, it was also found that the solubility ranking of ribavirin is not completely consistent with the absolute value of solvation free energy. Besides, the solubility ranking is not entirely following the principle of "like dissolves like" according to the polarity of the solvents selected in Table 4. Therefore, it is not enough to explain the solubility difference only by the polarity of the solvent and solvation free energy. Other factors, such as the size of solute molecules, viscosity, the ability of hydrogen bond formation, and solute–solvent interaction should also be considered.[34].

Ribavirin has 7 hydrogen bond acceptors and 4 hydrogen bond donors according to its molecular structure, which means that ribavirin is easy to form H-bonds interactions with solvent molecules, which could probably enhance the solubility in the relative solvents. For example, it can be seen from Table 4 that the polarity of dimethylacetamide is smaller than that of dimethylformamide. However, dimethylacetamide has larger hydrogen bond donor/acceptor propensities than dimethylformamide, which means that it is easier to form hydrogen bonds with ribavirin molecules. As a result, ribavirin has larger solubility in dimethylacetamide.

In addition, cohesive energy density is also a factor that should be considered. The cohesive energy density represents the solvent – solvent interaction, and a higher value of the cohesive energy density usually means a lower solubility.[35] It can be seen from Table 4 that water has a much larger cohesive energy density than *n*-methylpyrrolidone, dimethylacetamide, and dimethylformamide, which may be the reason why the solubility of ribavirin is smaller in water, even though it has a larger polarity.

In addition, the solubility date of ribavirin in alcohol solvents measured in this work and ref. [11] were compared in Fig. 8. The average solubility values of these alcohol solvents are ranked as ethylene glycol > 1,2-propanediol > methanol > ethanol > *n*-propanol ≈ *n*-butanol ≈ *sec*-butanol. It can be concluded that the solubility order of these alcohol solvents follows the "like dissolves like" rule, according to the polarity of these solvents. Furthermore, among the six solvents selected in this work, ribavirin has the lowest solubility in ethylene

Table 5
Parameters and deviations of the modified Apelblat equation for crystalline ribavirin (Form II) in six pure solvents at 0.1 MPa and 9.0 MPa.[a,b,c,d]

Parameters	*A*	*B*	*C*	ARD%	10^4RMSD
$p = 0.1$ MPa					
Water	−369.3528	12311.48	56.78372	3.032	6.187
Ethylene glycol	−601.8619	24276.25	90.51459	2.826	4.721
1,2-propanediol	−497.7571	19376.58	74.99456	2.756	2.125
N-methylpyrrolidone	−180.5561	7487.526	26.88673	0.2363	3.177
Dimethylformamide	−309.9813	12849.21	46.30094	0.8211	4.575
Dimethylacetamide	−50.15074	1521.722	7.468602	0.5348	6.267
Average ARD%	1.701				
Average 10^4RMSD	4.509				
$p = 9.0$ MPa					
Water	−448.2816	15942.70	68.48044	1.987	3.786
Ethylene glycol	−541.0542	21549.82	81.43910	2.162	3.342
1,2-propanediol	−544.0801	21595.83	81.80997	1.837	1.448
N-methylpyrrolidone	−174.2154	7218.079	25.93076	0.4054	5.368
Dimethylformamide	−287.9073	11864.98	42.99887	0.3782	2.132
Dimethylacetamide	−16.24978	22.68963	2.396608	0.1753	1.648
Average ARD%	1.157				
Average 10^4RMSD	2.954				

[a] The *A*, *B*, and *C* are model parameters in the Apelblat equation, which were calculated by correlating the experimental data.
[b] The ARD% and RMSD were calculated by Eqs. (18–19).
[c] Standard uncertainty of pressure at 0.1 MPa is $u(p) = 0.3$ kPa.
[d] Standard uncertainty of pressure at 9.0 MPa is $u(p) = 50$ kPa.

Table 6
Parameters and deviations of the NRTL model for crystalline ribavirin (Form II) in six pure solvents at 0.1 MPa and 9.0 MPa.[a,b,c,d]

Parameters	$10^{-3}\Delta g_{12}$	$10^{-3}\Delta g_{21}$	α	ARD%	10^4RMSD
$p = 0.1$ MPa					
Water	1.610271	−5.528645	0.47	3.772	4.633
Ethylene glycol	−20.63931	37.10672	0.08	2.635	3.169
1,2-propanediol	−9.823092	20.56538	0.20	11.27	5.655
N-methylpyrrolidone	−84.61452	108.6666	0.01	0.4489	6.206
Dimethylformamide	−54.54790	77.83411	0.02	0.6855	4.849
Dimethylacetamide	−83.41911	107.4731	0.01	2.205	21.32
Average ARD%	3.503				
Average 10^4RMSD	7.638				
$p = 9.0$ MPa					
Water	1.776528	−5.317712	0.47	5.716	6.408
Ethylene glycol	−20.65720	37.27909	0.08	2.131	2.551
1,2-propanediol	−10.06301	21.77155	0.20	12.60	6.100
N-methylpyrrolidone	−85.03550	109.6076	0.01	0.6127	9.309
Dimethylformamide	−54.63281	78.14891	0.02	0.7624	4.425
Dimethylacetamide	−83.96056	108.6915	0.01	2.600	24.45
Average ARD%	4.070				
Average 10^4RMSD	8.874				

[a] The Δg_{12}, Δg_{21}, and α are model parameters in the NRTL model, which were calculated by correlating the experimental data.
[b] The ARD% and RMSD were calculated by Eqs. (18–19).
[c] Standard uncertainty of pressure at 0.1 MPa is $u(p) = 0.3$ kPa.
[d] Standard uncertainty of pressure at 9.0 MPa is $u(p) = 50$ kPa.

glycol and 1,2-propanediol, which means ribavirin has excellent solubility in these solvents.

It is worth noting that the solubility of ribavirin (Form II) in water at 298.15 K reported by Goodarzi[37] and Chen[38] was 0.0103, and this value reported by Vasa [5] was 0.0108, which is very close to our results (0.0109). However, in ref. [10] and ref. [11], this value were 0.0174 and 0.0144, respectively, which deviates greatly from our results. The deviations of solubility between this work and refs. [10,11] are compared in Fig. 9. The difference may be caused by the determination method, equilibrium time, raw material purity, separation and analysis method, etc. Specifically, the concentration of ribavirin in water was analyzed by HPLC in ref. [10], in which the dilution operation may also cause additional deviation. The experimental device in ref. [11] was a 20 ml cylindrical bottle, while in this work a 100 ml crystallizer was used. The smaller amount of saturated solution in ref. [11] may further cause the deviation in solubility measurement.

4.3. Correlation of solubility data

The solubility data of ribavirin under two pressures were correlated by the modified Apelblat and NRTL models. The average relative deviation (ARD%) and the root-mean-square deviations (RMSD) were calculated to evaluate the applicability of the above two models under two pressures. The values of ARD% and RMSD can be calculated by Eqs. (18–19).[28].

$$\mathrm{ARD\%} = \frac{100}{N}\sum_{i=1}^{N}\left|\frac{x_i^{exp} - x_i^{cal}}{x_i^{exp}}\right| \tag{18}$$

$$\mathrm{RMSD} = \left[\frac{1}{N}\sum_{i=1}^{N}\left(x_i^{exp} - x_i^{cal}\right)^2\right]^{1/2} \tag{19}$$

where (x_i^{exp}-x_i^{cal}) represent the deviation between the experimental and calculated mole fraction solubility of ribavirin at the same temperature.

Table 7
The mixing thermodynamic properties of crystalline ribavirin (Form II) in six pure solvents at 0.1 MPa and 9.0 MPa.[a,b,c]

T(K)	p = 0.1 MPa			p = 9.0 MPa		
	$\Delta_{mix}G$	$\Delta_{mix}S$	$\Delta_{mix}H$	$\Delta_{mix}G$	$\Delta_{mix}S$	$\Delta_{mix}H$
Water						
283.15	−103.07	26.097	7.2864	−92.453	22.362	6.2393
288.15	−118.09	29.962	8.5156	−111.40	27.179	7.7204
293.15	−147.15	37.918	10.969	−135.46	33.426	9.6633
298.15	−196.17	51.986	15.304	−180.75	45.850	13.490
303.15	−252.15	68.512	20.517	−215.20	55.222	16.525
308.15	−315.79	87.815	26.745	−283.15	74.916	22.802
313.15	−413.14	118.88	36.814	−357.79	97.204	30.082
318.15	−519.54	154.07	48.499	−466.81	131.49	41.365
323.15	−639.57	195.26	62.460	−581.10	168.72	53.941
Ethylene glycol						
283.15	−121.87	219.76	62.102	−113.42	203.60	57.535
288.15	−127.53	225.72	64.913	−121.71	215.16	61.876
293.15	−135.94	236.80	69.283	−130.67	227.56	66.578
298.15	−149.70	258.05	76.787	−144.00	248.14	73.839
303.15	−179.16	310.13	93.838	−170.17	293.82	88.902
308.15	−217.68	380.28	116.96	−207.76	362.29	111.43
313.15	−252.73	442.87	138.43	−234.61	408.19	127.59
318.15	−290.04	509.57	161.83	−272.24	475.76	151.09
323.15	−339.69	601.75	194.12	−320.85	565.99	182.58
1,2-propanediol						
283.15	−51.778	60.463	17.068	−50.766	63.241	17.856
288.15	−54.868	62.030	17.819	−53.933	65.125	18.712
293.15	−62.811	69.675	20.362	−61.599	73.035	21.349
298.15	−71.489	77.827	23.133	−69.531	80.871	24.042
303.15	−82.948	89.070	26.919	−80.680	92.670	28.012
308.15	−102.73	110.49	33.946	−92.673	105.10	32.293
313.15	−122.35	131.18	40.957	−112.56	127.87	39.931
318.15	−145.65	156.12	49.524	−136.04	155.22	49.247
323.15	−166.94	177.73	57.266	−154.32	174.59	56.263
N-methylpyrrolidone						
283.15	−1972.2	5075.3	1435.1	−1954.3	5086.0	1438.2
288.15	−1930.3	4954.5	1425.7	−1916.8	4977.9	1432.5
293.15	−1910.8	4893.8	1432.7	−1887.2	4890.6	1431.8
298.15	−1906.9	4875.2	1451.6	−1867.8	4830.9	1438.5
303.15	−1902.5	4854.6	1469.8	−1878.2	4852.9	1469.3
308.15	−1925.8	4909.1	1510.8	−1901.1	4908.9	1510.8
313.15	−1960.1	4993.2	1561.7	−1921.4	4957.5	1550.5
318.15	−1978.0	5032.2	1599.0	−1952.3	5035.1	1600.0
323.15	−2018.7	5133.0	1656.7	−1967.6	5069.0	1636.1
Dimethylformamide						
283.15	−796.32	2010.8	568.56	−758.36	1919.5	542.74
288.15	−780.48	1956.7	563.05	−746.74	1877.4	540.22
293.15	−779.87	1944.3	569.20	−751.70	1880.8	550.61
298.15	−797.69	1982.3	590.22	−770.06	1921.0	571.97
303.15	−827.55	2053.1	621.56	−790.03	1965.2	594.96
308.15	−862.40	2137.4	657.77	−821.42	2040.8	628.05
313.15	−901.62	2233.5	698.52	−861.54	2140.5	669.43
318.15	−948.60	2350.9	747.00	−897.46	2228.2	708.01
323.15	−993.48	2462.3	794.70	−951.15	2365.5	763.47
Dimethylacetamide						
283.15	−1445.7	3682.8	1041.3	−1405.2	3631.5	1026.8
288.15	−1459.9	3714.0	1068.7	−1418.0	3661.1	1053.5
293.15	−1472.6	3740.5	1095.1	−1430.9	3690.5	1080.4
298.15	−1483.8	3762.6	1120.3	−1434.6	3694.1	1100.0
303.15	−1498.0	3792.7	1148.3	−1446.2	3719.5	1126.1
308.15	−1505.1	3802.6	1170.3	−1452.2	3728.8	1147.6
313.15	−1509.8	3805.5	1190.2	−1468.1	3765.4	1177.7
318.15	−1524.1	3834.7	1218.5	−1475.7	3778.5	1200.7
323.15	−1573.5	3960.6	1278.3	−1481.0	3784.6	1221.5

[a] The $\Delta_{mix}G$, $\Delta_{mix}H$ and $\Delta_{mix}S$ were calculated by Eqs. (8–10).
[b] The combined expanded uncertainties U are $Uc(\Delta H_m) = 0.060\Delta H_m$, $Uc(\Delta S_m) = 0.065\Delta S_m$, $Uc(\Delta G_m) = 0.065\Delta G_m$ (0.95 level of confidence).
[c] $\Delta_{mix}G$, $\Delta_{mix}S$, $\Delta_{mix}H$ in the unit of J·mol^{-1}, J·K^{-1}·mol^{-1}, kJ·mol^{-1}, respectively.

N is the number of experimental data points, which was taken as 9 in this paper.

The values of ARD% and RMSD were used to evaluate the correlation effect of the two models, which are listed in Tables 5-6, together with the model parameters. It was supposed that the ARD% of both models in nearly all of the solvents is less than 5 %, which means that, both models can give satisfactory results in the experimental pressure range. Only for the solubility of ribavirin in 1,2-propanediol, the correlation effect of the NRTL model is not satisfactory. Besides, the modified Apelblat model can give better correlation results because its ARD% value is lower than the NRTL models. This shows that the model is still available under a certain pressure range.

4.4. Mixing and dissolution thermodynamic properties

The thermodynamic properties in the process of mixing and

Table 8
The dissolution thermodynamic properties of crystalline ribavirin (Form II) in six pure solvents at 0.1 MPa and 9.0 MPa.[a,b,c].

T(K)	p = 0.1 MPa			p = 9.0 MPa		
	$\Delta_{dis}G$	$\Delta_{dis}S$	$\Delta_{dis}H$	$\Delta_{dis}G$	$\Delta_{dis}S$	$\Delta_{dis}H$
Water						
283.15	−10.071	26.688	7.5467	−8.8721	22.893	6.4732
288.15	−14.447	30.642	8.8151	−12.730	27.827	8.0055
293.15	−19.962	38.781	11.349	−17.730	34.224	10.015
298.15	−27.270	53.172	15.826	−24.241	46.949	13.974
303.15	−36.841	70.079	21.208	−32.794	56.550	17.110
308.15	−49.243	89.828	27.631	−43.985	76.722	23.598
313.15	−65.153	121.61	38.017	−58.328	99.553	31.117
318.15	−85.311	157.62	50.061	−76.530	134.67	42.770
323.15	−110.64	199.77	64.444	−99.438	172.82	55.748
Ethylene glycol						
283.15	−12.260	220.45	62.409	−11.686	204.24	57.820
288.15	−14.103	226.46	65.241	−13.421	215.87	62.189
293.15	−16.287	237.62	69.641	−15.505	228.34	66.922
298.15	−18.919	258.97	77.192	−18.018	249.03	74.229
303.15	−22.167	311.28	94.341	−21.097	294.91	89.380
308.15	−26.062	381.72	117.60	−24.786	363.68	112.04
313.15	−30.905	444.61	139.20	−29.425	409.80	128.30
318.15	−36.960	511.63	162.74	−35.145	477.69	151.94
323.15	−44.560	604.26	195.22	−42.332	568.36	183.62
1,2-propanediol						
283.15	−3.6503	60.768	17.203	−3.3233	63.542	17.989
288.15	−4.9518	62.358	17.963	−4.5148	65.450	18.855
293.15	−6.3524	70.058	20.531	−5.7822	73.413	21.515
298.15	−8.1123	78.272	23.329	−7.3942	81.307	24.234
303.15	−10.283	89.598	27.151	−9.3609	93.189	28.241
308.15	−12.965	111.17	34.245	−11.846	105.71	32.562
313.15	−16.429	132.01	41.323	−14.956	128.64	40.268
318.15	−20.846	157.14	49.973	−18.959	156.17	49.668
323.15	−26.407	178.93	57.793	−24.004	175.70	56.752
N-methylpyrrolidone						
283.15	−271.49	5086.1	1439.9	−265.56	5096.8	1442.9
288.15	−271.97	4965.3	1430.5	−265.08	4988.7	1437.2
293.15	−274.76	4904.9	1437.6	−267.17	4901.6	1436.6
298.15	−279.90	4886.6	1456.7	−271.73	4842.1	1443.4
303.15	−287.75	4866.3	1474.9	−278.37	4864.6	1474.4
308.15	−297.74	4921.4	1516.2	−287.40	4921.1	1516.2
313.15	−310.29	5006.1	1567.4	−299.32	4970.3	1556.1
318.15	−326.36	5045.7	1605.0	−313.96	5048.5	1605.9
323.15	−345.08	5147.3	1663.0	−332.30	5082.9	1642.2
Dimethylformamide						
283.15	−82.114	2015.3	570.56	−78.410	1923.8	544.64
288.15	−83.977	1961.3	565.06	−80.093	1881.7	542.14
293.15	−86.969	1949.0	571.27	−82.856	1885.3	552.60
298.15	−91.089	1987.2	592.40	−86.707	1925.8	574.08
303.15	−96.413	2058.4	623.91	−91.790	1970.3	597.20
308.15	−103.11	2143.1	660.30	−98.145	2046.3	630.46
313.15	−111.38	2239.7	701.25	−105.96	2146.4	672.04
318.15	−121.43	2357.7	749.98	−115.58	2234.6	710.83
323.15	−133.65	2469.6	797.92	−127.09	2372.5	766.56
Dimethylacetamide						
283.15	−190.24	3690.8	1044.9	−182.27	3639.2	1030.3
288.15	−191.31	3722.3	1072.4	−182.53	3669.2	1057.1
293.15	−194.25	3749.2	1098.9	−184.59	3699.0	1084.2
298.15	−199.21	3771.6	1124.3	−188.72	3702.9	1103.8
303.15	−206.21	3802.1	1152.4	−194.75	3728.6	1130.1
308.15	−215.59	3812.4	1174.6	−203.05	3738.2	1151.7
313.15	−227.37	3815.6	1194.6	−213.41	3775.2	1182.0
318.15	−241.42	3845.2	1223.1	−226.32	3788.7	1205.1
323.15	−257.59	3971.8	1283.2	−241.77	3795.1	1226.1

[a] The $\Delta_{dis}G$, $\Delta_{dis}H$ and $\Delta_{dis}S$ were calculated by Eqs. (14–16).
[b] The combined expanded uncertainties U are $Uc(\Delta H_m) = 0.060\Delta H_m$, $Uc(\Delta S_m) = 0.065\Delta S_m$, $Uc(\Delta G_m) = 0.065\Delta G_m$ (0.95 level of confidence).
[c] $\Delta_{dis}G$, $\Delta_{dis}S$, $\Delta_{dis}H$ in the unit of J·mol^{-1}, J·K^{-1}·mol^{-1}, kJ·mol^{-1}, respectively.

dissolution under high pressure must be different from those under atmospheric pressure. Therefore, the mixing and dissolution thermodynamic properties of ribavirin under two pressures were calculated based on the experimental solubility values and the NRTL model and were listed in Tables 7-8. It was found that $\Delta_{mix}G$ and $\Delta_{dis}G$ are negative, and $\Delta_{mix}H$, $\Delta_{dis}H$, $\Delta_{mix}S$, and $\Delta_{dis}S$ are positive, suggesting that both the mixing and dissolution processes under two pressures are spontaneous, endothermic, and entropy-driving. Furthermore, the absolute values of $\Delta_{dis}G$, $\Delta_{dis}S$, and $\Delta_{dis}H$ under 9.0 MPa are slightly lower than that under 0.1 MPa, which is consistent with the results that the solubility data of ribavirin is lower under 9.0 MPa.

5. Conclusions

The solubility of ribavirin in six pure solvents was measured from 283.15 K to 323.15 K, under 9.0 MPa and 0.1 MPa respectively. It was

suggested that the solubility in each solvent decreased slightly under 9.0 MPa compared with that under 0.1 MPa, and the decreasing trend is more obvious with the temperature rising. Besides, it was found that the effect of temperature was stronger compared with pressure. The solubility data in each solvent increased significantly with the temperature rising, and the average solubility values in the entire experimental temperature range are ranked as *n*-methylpyrrolidone > dimethylacetamide > dimethylformamide > water > ethylene glycol > 1,2-propanediol. Moreover, the experimental solubility data under two pressures were correlated by the modified Apelblat equation and the NRTL model. The results indicated that the above two models are still applicable in a certain pressure range. And the modified Apelblat equation can give better correlation results with Average relative deviation (ARD%) values lower than 2 %. Finally, the calculation results of thermodynamic properties suggested that both the mixing and the dissolution processes under two pressures are endothermic, spontaneous, and driven by entropy in the experimental solvent systems. The absolute values of $\Delta_{dis}G$ under 9.0 MPa are lower than those under atmospheric pressure, which is consistent with the decrease of solubility under high pressure.

CRediT authorship contribution statement

Yaoguang Feng: Conceptualization, Methodology, Validation, Data curation, Writing – original draft. **Hongxun Hao:** Conceptualization, Validation, Funding acquisition. **Beiqian Tian:** Software. **Kui Chen:** Investigation. **Na Wang:** Visualization. **Ting Wang:** Formal analysis, Writing – review & editing, Supervision. **Xin Huang:** Validation, Resources, Writing – review & editing, Project administration.

Declaration of Competing Interest

The authors declare that they have no known competing financial interests or personal relationships that could have appeared to influence the work reported in this paper.

Data availability

No data was used for the research described in the article.

Acknowledgment

This research is financially supported by the National Natural Science Foundation of China (grants 21978201 and 21908159).

Appendix A. Supplementary data

Supplementary data to this article can be found online at https://doi.org/10.1016/j.jct.2022.106897.

References

[1] S. Crotty, C. Cameron, R. Andino, Ribavirin's antiviral mechanism of action: lethal mutagenesis? J. Mol. Med. 80 (2) (2002) 86–95.
[2] J.-M. Chen, S. Li, T.-B. Lu, Pharmaceutical Cocrystals of Ribavirin with Reduced Release Rates, Cryst. Growth Des. 14 (12) (2014) 6399–6408.
[3] D.M. Vasa, Z. Bakri, M.D. Donovan, L.A. O'Donnell, P.L.D. Wildfong, Evaluation of Ribavirin-Poloxamer Microparticles for Improved Intranasal Absorption, Pharmaceutics 13 (8) (2021) 1126.
[4] V. Sakharov, S. Baykov, I. Konstantinova, R. Esipov, M. Dorogov, An Efficient Chemoenzymatic Process for Preparation of Ribavirin, Int. J. Chem. Eng. 2015 (2015), 734851.
[5] D.M. Vasa, P.L.D. Wildfong, Solid-state transformations of ribavirin as a result of high-shear mechanical processing, Int. J. Pharm. 524 (1) (2017) 339–350.
[6] P. Prusiner, M. Sundaralingam, The crystal and molecular structures of two polymorphic crystalline forms of virazole (1-[beta]-d-ribofuranosyl-1,2,4-triazole-3-carboxamide). A new synthetic broad sprectrum antiviral agent, Acta Crystallograph. Sect. B. 32 (2) (1976) 419–426.
[7] H.H.Y. Tong, B.Y. Shekunov, J.P. Chan, C.K.F. Mok, H.C.M. Hung, A.H.L. Chow, An improved thermoanalytical approach to quantifying trace levels of polymorphic impurity in drug powders, Int. J. Pharm. 295 (1) (2005) 191–199.
[8] J. Weng, Y. Huang, D. Hao, Y. Ji, Recent advances of pharmaceutical crystallization theories, Chin. J. Chem. Eng. 28 (4) (2020) 935–948.
[9] Q. Liu, J. Wang, H. Wu, S. Zong, Y. Zhou, H. Hao, X. Huang, Thermodynamic models for determination of solid-liquid equilibrium of the 4-methoxybenzoic acid in different solvents with solubility parameters and interaction energy aided analyses, J. Mol. Liq. 330 (2021), 115669.
[10] X. Li, Y. Cong, W. Li, P. Yan, H. Zhao, Thermodynamic modelling of solubility and preferential solvation for ribavirin (II) in co-solvent mixtures of (methanol, n-propanol, acetonitrile or 1,4-dioxane)+water, J. Chem. Thermodyn. 115 (2017) 74–83.
[11] Q. Li, L. Zhou, S. Zhang, K. Shi, J. Dai, H. Wang, Q. Yin, Z. Wang, Measurement and Correlation of the Solubility and Thermodynamic Properties of Ribavirin(II) in Nine Pure Solvents and (1-Propanol + Water) Binary Solvents, J. Chem. Eng. Data 66 (10) (2021) 3713–3721.
[12] N.T. Morgan, T.C. Frank, R.J. Holmes, E.L. Cussler, Effect of Rapid Pressurization on the Solubility of Small Organic Molecules, Cryst. Growth Des. 16 (3) (2016) 1404–1408.
[13] S. Sawamura, N. Yoshimoto, Y. Taniguchi, Y. Yamaura, Effects of pressure and temperature on the solubility of ammonium chloride in water, High Pressure Res. 16 (4) (1999) 253–263.
[14] C. Pando, A. Cabañas, I.A. Cuadra, Preparation of pharmaceutical co-crystals through sustainable processes using supercritical carbon dioxide: a review, RSC Adv. 6 (75) (2016) 71134–71150.
[15] A.A.F. Zielinski, A.d.P. Sanchez-Camargo, L. Benvenutti, D.M. Ferro, J.L. Dias, S.R. S. Ferreira, High-pressure fluid technologies: Recent approaches to the production of natural pigments for food and pharmaceutical applications, Trends Food Sci. Technol. 118 (2021) 850–869.
[16] Z. Wu, S. Yang, W. Wu, Application of temperature cycling for crystal quality control during crystallization, CrystEngComm 18 (13) (2016) 2222–2238.
[17] E. Sheikholeslamzadeh, C.-C. Chen, S. Rohani, Optimal Solvent Screening for the Crystallization of Pharmaceutical Compounds from Multisolvent Systems, Ind. Eng. Chem. Res. 51 (42) (2012) 13792–13802.
[18] R. Sabbah, A. Xu-wu, J.S. Chickos, M.L.P. Leitão, M.V. Roux, L.A. Torres, Reference materials for calorimetry and differential thermal analysis, Thermochim Acta 331 (2) (1999) 93–204.
[19] Y. Zhou, J. Wang, T. Wang, J. Gao, X. Huang, H. Hao, Solubility and dissolution thermodynamic properties of L-carnosine in binary solvent mixtures, J. Chem. Thermodyn. 149 (2020), 106167.
[20] N. Wei, Z. Shang, N. Zhang, J. Wang, S. Wu, Deep analysis of the solubility behaviour mechanism of alpha-(trichloromethyl) benzyl acetate in three binary aqueous solvents, J. Chem. Thermodyn. 151 (2020), 106246.
[21] N. Hansen, W.F. van Gunsteren, Practical Aspects of Free-Energy Calculations: A Review, J. Chem. Theory Comput. 10 (7) (2014) 2632–2647.
[22] L. Jia, J. Yang, P. Cui, D. Wu, S. Wang, B. Hou, L. Zhou, Q. Yin, Uncovering solubility behavior of Prednisolone form II in eleven pure solvents by thermodynamic analysis and molecular simulation, J. Mol. Liq. 342 (2021), 117376.
[23] Y. Zhou, D. Han, T. Tao, S. Zhang, J. Wang, J. Gong, Y. Wang, Solubility measurement, thermodynamic correlation and molecular simulations of uracil in (alcohol + water) binary solvents at (283.15–318.15) K, J. Mol. Liq. 318 (2020), 114259.
[24] J. Li, X. Ji, C. Li, Z. Li, D. Wu, B. Zhang, B. Hou, L. Zhou, C. Xie, J. Gong, W. Chen, Solubility measurement and thermodynamic correlation of (2,4-dichlorophenoxy) acetic acid in fifteen pure solvents, J. Chem. Thermodyn. 163 (2021), 106589.
[25] S. Yu, W. Xing, F. Xue, Y. Cheng, B. Li, Solubility and thermodynamic properties of nimodipine in pure and binary solvents at a series of temperatures, J. Chem. Thermodyn. 152 (2021), 106259.
[26] S. Baluja, A. Hirapara, Solubility and solution thermodynamics of novel pyrazolo chalcone derivatives in various solvents from 298.15 K to 328.15 K, J. Mol. Liq. 277 (2019) 692–704.
[27] J. Ma, X. Huang, N. Wang, X. Li, Y. Bao, T. Wang, H. Hao, Solubility and thermodynamic mixing and dissolution properties of empagliflozin in pure and binary solvent systems, J. Mol. Liq. 309 (2020), 113004.
[28] S. Guo, W. Su, H. Hao, Y. Luan, X. Li, S. Gao, X. Huang, Solution Thermodynamics of Caprolactam in Different Monosolvents, J. Chem. Eng. Data 66 (1) (2021) 494–503.
[29] Y. Zhang, H. Hao, N. Wang, C. Xie, Q. Yin, X. Huang, Solubility and dissolution thermodynamic properties of 1,6-Bis[3-(3,5-di-tert-butyl-4-hydroxyphenyl)propionamido]hexane in pure solvents and binary solvent mixtures, J. Mol. Liq. 252 (2018) 103–111.
[30] K. Moodley, J. Rarey, D. Ramjugernath, Experimental solubility of diosgenin and estriol in various solvents between T=(293.2–328.2)K, J. Chem. Thermodyn. 106 (2017) 199–207.
[31] R. Orye, J. Prausnitz, Multicomponent equilibria with the Wilson equation, Ind. Eng. Chem. 57 (1965).
[32] F. Liu, H. Qu, X. Wan, D. Han, W. Li, S. Wu, Solubility and Data Correlation of β-Arbutin in Different Monosolvents from 283.15 to 323.15 K, J. Chem. Eng. Data 64 (12) (2019) 5688–5697.
[33] K. Kawakami, Ultraslow Cooling for the Stabilization of Pharmaceutical Glasses, J. Phys. Chem. B 123 (23) (2019) 4996–5003.
[34] D. Han, X. Li, H. Wang, Y. Wang, S. Du, B. Yu, Y. Liu, S. Xu, J. Gong, Determination and correlation of pyridoxine hydrochloride solubility in different binary mixtures

at temperatures from (278.15 to 313.15)K, J. Chem. Thermodyn. 94 (2016) 138–151.
[35] C.H. Gu, H. Li, R.B. Gandhi, K. Raghavan, Grouping solvents by statistical analysis of solvent property parameters: implication to polymorph screening, Int. J. Pharm. 283 (1–2) (2004) 117–125.
[36] Y. Marcus, The Properties of Solvents, Wiley, Chichester; New York, 1998.
[37] N. Goodarzi, A. Barazesh Morgani, B. Abrahamsson, R. Cristofoletti, D.W. Groot, P. Langguth, M.U. Mehta, J.E. Polli, V.P. Shah, J.B. Dressman, Biowaiver Monographs for Immediate Release Solid Oral Dosage Forms: Ribavirin, J. Pharm. Sci. 105 (4) (2016) 1362–1369.
[38] J.-M. Chen, S. Li, T.-B. Lu, Pharmaceutical Cocrystals of Ribavirin with Reduced Release Rates, Cryst. Growth Des. 14 (2014) 6399, https://doi.org/10.1021/cg501247x.